IEEE Access
Multidisciplinary | Rapid Review | Open Access Journal

Received 15 March 2023, accepted 30 March 2023, date of publication 3 April 2023, date of current version 10 April 2023.

Digital Object Identifier 10.1109/ACCESS.2023.3264263

RESEARCH ARTICLE

Global Prescribed Performance-Based Fault-Tolerant Control for Trajectory Tracking of the ACV With Uncertainty

MINGYU FU, DAN BAI, AND HANBO DENG
College of Automation, Harbin Engineering University, Harbin 150001, China

Corresponding author: Dan Bai (baidan1990@hrbeu.edu.cn)

This work was supported in part by the Research Project funded by the "Research on Maneuverability of High Speed Hovercraft" under Project 2007DFR80320, and in part by the National Natural Science Foundation of China under Grant 51309062 and Grant 52071112.

ABSTRACT This paper focuses on a fixed-time prescribed performance-based Fault-tolerant controller that guarantees the global performance for the Trajectory tracking control of the air cushion vehicle (ACV). In the presence of faults, time-varying parameters and environmental disturbances, the proposed control system in this paper has good robustness and control performance. Firstly, an integrated observer for disturbances and faults is proposed to suppress all uncertainties in the system. Then a novel prescribed performance function is designed that does not need to be constrained by the initial value of the target errors while ensuring that it has fixed-time convergence performance. Global prescribed performance control has the advantage of separating the error initial conditions from the prescribed performance function. At the same time, combined with the global sliding mode control method, the fast convergence and robustness of the whole system are guaranteed. Finally, the simulation results verify the effectiveness of the control system.

INDEX TERMS Air cushion vehicle, prescribed performance control, trajectory tracking, fault-tolerant control.

I. INTRODUCTION

With the widespread use of the air cushion vehicle (ACV) in military and civilian applications [1], the fault-tolerant control systems for Trajectory tracking of the ACV is a hot topic of current research. The huge challenge of the tracking control system for amphibious ACV with unknown perturbations, unmodeled errors and fail-safe issues is mainly attributed to the high speeds, complex operating environment and special structures [2]. It is therefore urgent to design fault-tolerant control systems of the ACV with greater robustness reject unknown disturbance and fault, with fast response [3] and high precision of tracking errors.

The first concern focuses on the transient performance which excellent for the safe navigation of ACV. For achieving higher quality transient performance and high precision tracking errors, the prescribed performance control (PPC) [4], [5], [6] has been the focus of recent research by experts. This is attributed to its ability to ensure that the target error is restricted to a predefined set [10]. The prescribed performance function (PPF) guarantees the amount of overshoot of the system error and the rate of convergence to satisfy an arbitrarily small pre-designed region [11]. The [12] investigates an adaptive back stepping Trajectory tracking control system of dynamic positioning (DP) ships with the disturbance and input saturation. The control system combines PPC method and a disturbance observer (DO) to improve the control performance of the system. Based on a prescribed performance function, an adaptive fixed-time Trajectory tracking controller of the ACV with model uncertainties and environment disturbances is proposed by [13]. In [14], an adaptive fault-tolerant controller with a monitoring function is proposed for nonlinear systems with uncertain parameters and actuator failures, applying the PPC to guarantee the transient steady-state performance of the system. A novel fixed-time terminal sliding mode

The associate editor coordinating the review of this manuscript and approving it for publication was Zheng Chen.

(FxTTSM) with PPF is introduced by [15] to improve the transient and steady-state performance of the tracking of autonomous underwater vehicles (AUVs). However, the initial bound for the prescribed performance function in the above papers must satisfy the inequalities $-\alpha(0)\beta(0) < e(0) < \alpha(0)\beta(0)$ and $0 < \alpha(t) < 1$, where $\alpha(0)$ is the initial value of $\alpha(t)$, $e(0)$ and $\beta(0)$ are the initial values of the target error and performance function respectively. This constraint hinders the application of the PPC method to many complex practical engineering systems with substantial uncertainties and faults. For traditional PPC methods, The singular value problem arises when $e(0) = \beta(0)$. This paper uses a transformation error function with time-varying bounds, a variation that removes the initial value limitations of the PPC. Methods with above-mentioned advantages are defined as global prescribed performance functions. In contrast to [7] and [8], this paper and [3], [9], and [21] focuses more on the limiting problem of the initial values, and the problem of fragility after the onset of failure will be discussed further in future work. The finite-time [7] and fixed-time [6] convergence problem of transient performance is also essential for tracking systems. A fixed time convergence global PPC method is used in [3] and [21], but requires more special functions to implement.The method in this paper has more flexible structure.

The focus then has to be on ensuring robustness of the tracking control system for ACV under strong uncertainty. Non-linear disturbance observer (NDO) [16], [18] is also a better selection that was utilized to suppress uncertainty compared to the more computationally intensive neural network estimation methods. A terminal sliding mode controller in [19] with PPF based on the sliding mode disturbance observer (SMDO) of the extended state observer (ESO) is applied to the tracking system of the underwater vehicle. The fixed-time problem of transient performance is also essential for tracking systems. A fixed-time observer-based adaptive tracking controller with prescribed transient performance is proposed by [20] for underactuated unmanned underwater vehicles (UUV). In [21], a prescribed performance function with fixed time convergence is proposed, while the barrier Lyapunov function (BLF) is used to restrict the state error to the desired range. Despite the existing effective methods being used to estimate and suppress uncertainty in the system. Further improvements are still needed for non-linear ACV systems with strong uncertainties including information on faults, time-varying parameters and environmental disturbances. From the special physical structure and complex operating environment of ACV point of view, a more suitable observer requiring less perturbative information is more meaningful. An extended state observer is designed in [22] to ensure the robustness of the system by considering the Trajectory tracking control system of ACV with unknown perturbations.

Sliding-mode variational techniques are widely used in fault-tolerant tracking control systems due to their inherent robustness to uncertainties [17]. A based sliding mode and backstepping fault-tolerant control (FTC) scheme for the nonlinear systems with disturbances and actuator mismatch is proposed in [23]. A fixed-time sliding mode fault-tolerant controller in [24] is developed to compensate for the uncertain and actuator effectiveness faults of the robot system. In the research of perfecting sliding mode control methods, how to let the system state slide into a stable state with strong robustness as soon as possible is a hot topic of discussion in recent years. The global sliding mode control method [2], [25] was therefore created, due to its advantage of enabling states to be switched quickly. However, we have never ceased to enhance and improve the performance of the sliding mode variable structure. To better track the target, we have combined the sliding mode control with a pre-defined performance function, which ensures that the tracking error is limited to a pre-defined range for a limited time while still guaranteeing good robustness in the event of an actuator failure.

The focus control objective of this paper is to improve the transient and steady-state performance of fault-tolerant controller of the ACV tracking systems with strong uncertainties including fault information based on a novel prescribed performance function with a boundary function for finite-time convergence. For the whole control system, the specific contributions of this paper are as follows:

1) Analyzed from a global perspective, the PPC method in this paper solves the problem of constrained initial values, just like [3], [9], and [21]. The difference is that the solution in this paper is more general. References [3] and [21] used a special error transformation function such that the initial value of the performance boundary is infinity; But this transformation function is too special and lacks generality;
2) Compared with the traditional PPFs designed in [10], [11], [12], [13], [14], and [15], a new PPC method with time-varying bounds that is not constrained by the initial conditions is proposed in this paper. Transformation errors do not require normalization as [3], let alone special transformation functions. The improved prescribed performance including fixed-time convergence and high steady-state error accuracy;
3) A new global sliding mode surface is used to ensure that the error transformation function enters the sliding mode initially, giving the system a high degree of robustness while ensuring performance in tracking error transients;
4) In the presence of uncertainty and faults, ACV's tracking control system, with a combination of controller and integrated observer, ensures that the tracking and state errors converge to near the origin in a fixed amount of time.

The problem description of the tracking control model of ACV and some prior knowledge is presented in Section II. Section III describes the design and analysis of the observer and controller for this paper in detail. Numerical simulation results are presented in Section IV. Section V offers a brief conclusion of the article.

II. PROBLEM DESCRIPTION AND PREPARATORY KNOWLEDGE

A. PROBLEM DESCRIPTION

Based on the earth coordinate and the body coordinate reference frame, the kinematics and dynamics of the ACV can be described as:

$$\begin{aligned}\dot{\boldsymbol{\eta}} &= \boldsymbol{R}(\varphi, \psi)\boldsymbol{v} \\ \dot{\boldsymbol{v}} &= \boldsymbol{M}^{-1}\boldsymbol{C}(\boldsymbol{v})\boldsymbol{v} + \boldsymbol{M}^{-1}\boldsymbol{F}(\boldsymbol{v}) + \boldsymbol{B}\boldsymbol{\tau} + \boldsymbol{D}(\boldsymbol{v}, \boldsymbol{\eta})\end{aligned} \tag{1}$$

where $\boldsymbol{M} = diag\{m, m, I_x, I_z\}$ is the inertia matrix and $\boldsymbol{C}(\boldsymbol{v})$ is the Coriolis matrix. $\boldsymbol{F}(\boldsymbol{v})$ is the known total drags are denoted by $\boldsymbol{F}(\boldsymbol{v}) = [F_u, F_v, F_p, F_r]^T$, the details can be obtained in [2]. $\boldsymbol{\eta} = [x, y, \varphi, \psi]^T$ is the position vector matrix of the earth-fixed frame, including the surge and sway position x, y, the roll and yaw angle φ, ψ. $\boldsymbol{v} = [u, v, p, r]^T$ is the body-fixed frame velocity vector matrix, u,v,p,r are the surge, sway, roll and yaw velocity of the ACV respectively. $\boldsymbol{B} = diag\{b_u, 0, 0, b_r\}$ is the health parameter matrix of the actuators, $\boldsymbol{\tau} = [\tau_u, 0, 0, \tau_r]^T$ is the input vector matrix of the air propellers and air rudders. The other matrixs in the above equation is described in detail as follows:

$$\boldsymbol{R}(\varphi, \psi) = \begin{bmatrix} \cos\psi & -\sin\psi\cos\varphi & 0 & 0 \\ \sin\psi & \cos\psi\cos\varphi & 0 & 0 \\ 0 & 0 & 1 & 0 \\ 0 & 0 & 0 & \cos\varphi \end{bmatrix} \tag{2}$$

$$\boldsymbol{C}(\boldsymbol{v}) = \begin{bmatrix} 0 & 0 & 0 & -mv \\ 0 & 0 & 0 & mu \\ 0 & 0 & 0 & 0 \\ 0 & 0 & 0 & 0 \end{bmatrix} \tag{3}$$

where $\boldsymbol{R}(\varphi, \psi)$ is the transformation matrix and $\boldsymbol{D}(\boldsymbol{v}, \boldsymbol{\eta}) = [d_u, d_v, d_p, d_r]^T$ is the external disturbance matrix.

Remark 1: The $\boldsymbol{F}(\boldsymbol{v})$ in the above equation is described as the combined force of all hydro-air drag forces received by the ACV, assuming that $\boldsymbol{F}(\boldsymbol{v})$ is available from actual ship experiments. The unavailable dynamical part, which in this paper we combine with external disturbances, is collectively referred to here as the uncertain dynamics part of the ACV and described by the matrix $\boldsymbol{D}(\boldsymbol{v}, \boldsymbol{\eta})$, which includes the variable parameters, external disturbances, and the unmodelled error. A detailed description of the hydro-air resistance of hovercraft can refer to the [2].

To facilitate the design of the observer controller below, we have rewritten system (1) in the following form:

$$\begin{aligned}\dot{\boldsymbol{\eta}} &= \boldsymbol{R}(\varphi, \psi)\boldsymbol{v} \\ \boldsymbol{t}v &= \boldsymbol{A}\boldsymbol{v} + f(\boldsymbol{\eta}, \boldsymbol{v}) + \boldsymbol{B}_x\boldsymbol{\tau} + \boldsymbol{\xi}\end{aligned} \tag{4}$$

from system (1) and the transformed system (4), we can know $B_x = R(\varphi, \psi)M^{-1}B, f(\boldsymbol{\eta}, \boldsymbol{v}) = R(\varphi, \psi)M^{-1}(C(v)+F(v))+\dot{R}v$ and $\boldsymbol{\xi} = RD(v, \eta)$. The fault information of the system is described as

$$\boldsymbol{\tau}_j^f = diag\{b_j\}\boldsymbol{\tau}, t > t_j \tag{5}$$

where b_j stands for the health efficiency parameters of the actuator. $b_j = 1$ represents the j-th actuator is fault-free, means $\boldsymbol{\tau}_j^f = \boldsymbol{B}_x\boldsymbol{\tau}$. $b_j \in \left[b_j^f, 1\right)$, $0 < b_j^f < 1$ represents the j-th actuator is no complete failure, occurring at time t_j, also defines there are j actuators failed during time period $t^{j+1} = \left[t_j, t_{j+1}\right)$, and $j < m$. $\boldsymbol{\tau}_j^f \leq \boldsymbol{B}_x\boldsymbol{\tau}, j = 1, 2, 3, 4$.

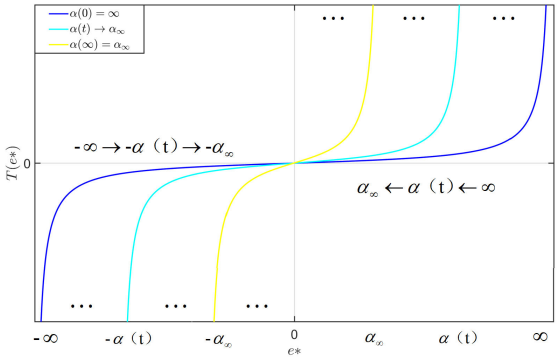

FIGURE 1. Prescribed performance error transfer function.

B. PREPARATORY KNOWLEDGE

Lemma 1: [27] Consider the vector $V(t)$ is continuously differentiable. If it's derivative satisfies

$$\dot{V}(t) = -a_v V^p(t) - b_v V^q(t) \tag{6}$$

where $a_v > 0$, $b_v > 0$, $0 < q < 1$, $p > 1$, Then, the system (5) is Fixed-time Stability, where the system can convergence in the setting time $t_{max} = \frac{1}{a_v(1-q)} + \frac{1}{b_v(p-1)}$, $\forall V(0) \in R^n$.

Lemma 2: [28] demonstrated that when the global sliding mode controller meets the following conditions, the target error e_x can be converged to near the origin in a finite time and has global robustness. The sliding surface is designed as:

$$S = \dot{e}_x + \partial e_x - f(t) \tag{7}$$

where ∂ is positive constant, the forcing function $f(t)$ must be satisfy three conditions: (1)$f(0) = \dot{e}_x(0) + \partial e_x(0)$; (2) When $t \to \infty$, then $f(t) \to 0$; (3) $\dot{f}(t)$ is the derivative of $f(t)$ exists and is continuous.

Lemma 3: [11] The prescribed performance funcion of the position error in [10] and [11] should satisfy the following inequality:

$$-\delta p(t) < \mathbf{e}_1 < \delta p(t), \forall t \geq 0, \tag{8}$$

where $0 < \delta \leq 1$, this is the general form of the prescribed performance funcion.

Remark 2: δ is fixed parameter in [10], [11], and [17] which is designed to take values between 0 and 1. However, for the whole PPC theory, this definition limits this method's widespread use and is unnecessary. The bounds in this paper have been designed as time-varying functions with no such restriction, convergence in finite time, and asymmetrical.

In summary, the following inequality relation is proposed in this paper,

$$-\underline{\delta}(t)p(t) < \mathbf{e}_1 < \overline{\delta}(t)p(t), \forall t \geq 0, \tag{9}$$

It is known from Remark 2 that the time-vary boundaries has the following features:

1) $\underline{\delta}(t) > 0, \overline{\delta}(t) > 0$ are decreasing functions.
2) $\begin{cases} \lim_{t\to\infty} \overline{\delta}(t) = \overline{\delta}_\infty \\ \lim_{t\to\infty} \underline{\delta}(t) = \underline{\delta}_\infty \end{cases}$

Remark 3: As can be seen from the above conditions, in comparison with [21], the initial value of the boundary does not need to be infinite and also does not require error normalization. Since the boundary is no longer fixed at a point, the singularity problem does not arise. This improvement is more conducive to applying the PPC method in practical engineering.

Next, based on the time-varying boundary function designed above, we had to develop a new time-varying error transformation function, different from the one in the paper [11], as:

$$S(z) = \frac{\mathbf{e}_1}{p(t)} \tag{10}$$

where the z_1 is the Transformation error, where $e_1^* = \frac{\mathbf{e}_1}{p(t)}$.

The conversion function $S(z)$ should satisfy the following conditions:

1) $S(z_1)$ is smooth, monotonically increasing in the domain of definition and has the inverse function $S^{-1}(z_1) = T(e_1^*) = z_1$.
2) $-\underline{\delta}(t) < S(z_1) < \overline{\delta}(t)$.
3) $\begin{cases} \lim_{z_1\to\infty} S(z_1) = \overline{\delta}(t) \\ \lim_{z_1\to-\infty} S(z_1) = -\underline{\delta}(t) \end{cases}$

Based on the above three conditions for the transformation error function, a novel barrier Liapunov function with variable boundaries is designed as follows:

$$T(e_1^*) = \begin{cases} \frac{e_1^*}{\overline{\delta}^2(t) - e_1^{*2}}, e_1^* \geq 0 \\ \frac{e_1^*}{\underline{\delta}^2(t) - e_1^{*2}}, e_1^* < 0 \end{cases} \tag{11}$$

Figs. 1 explains the theorem more visually.

Remark 4: It is diffferet the transformation error function $S(\mathbf{z}_1) = \frac{\overline{\delta}e^{(z_1+r)} - \underline{\delta}e^{(z_1+r)}}{e^{(z_1+r)} + e^{-(z_1+r)}}$ in [26]. This can be any function with the above properties and variable boundaries. Ultimately it is sufficient to show that the transformation error converges near the origin.

III. DESIGN AND ANALYSIS OF CONTROLLERS AND OBSERVERS

This section focuses on the design and analysis of the observer and the sliding mode controller. Firstly, the observer is used to estimate the uncertain part of the system, then the error is transformed in combination with a prescribed performance function, the sliding mode controller for the whole closed-loop system is described and finally the stability of the whole system and the validity of the prescribed performance function are demonstrated.

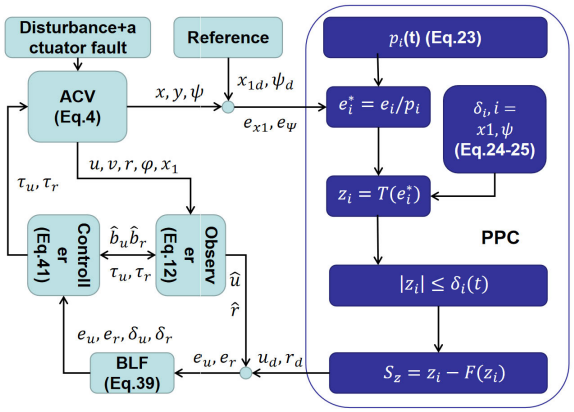

FIGURE 2. The structure diagram of the entire control system for Trajectory tracking of ACV.

A. INTEGRATED OBSERVE

To address the uncertainty of the system, this paper designs an observer that does not require perturbation of upper bound information to enhance the robustness of the system to disturbances and actuator failures. The observer is described in detail as follows,

$$\begin{aligned} \dot{\hat{\boldsymbol{v}}} &= \boldsymbol{A}\hat{\boldsymbol{v}} + f(\boldsymbol{\eta}, \boldsymbol{v}) + \hat{\boldsymbol{B}}_x\boldsymbol{\tau} + \hat{\boldsymbol{\xi}} + \boldsymbol{L}e_v \\ \hat{\boldsymbol{\xi}} &= \boldsymbol{z} + \boldsymbol{L}_\xi \boldsymbol{v} \\ \dot{\boldsymbol{z}} &= -\boldsymbol{L}_\xi(\dot{\hat{\boldsymbol{v}}} + \boldsymbol{A}e_v) + \delta \end{aligned} \tag{12}$$

where $e_v = \boldsymbol{v} - \hat{\boldsymbol{v}}$ and $e_\xi = \boldsymbol{\xi} - \hat{\boldsymbol{\xi}}$ are the errors of the velocity vector and system perturbations, $\hat{\boldsymbol{v}}$ and $\hat{\boldsymbol{\xi}}$ are the estimates of the observer. $\boldsymbol{L}$ and $\boldsymbol{L}_\xi$ are all positive definite matrixs. z is the intermediate variable of the observer and δ is the compensation function of the integrated observer and δ is described as follows

$$\delta = -\boldsymbol{k}_\xi \boldsymbol{L}_\xi e_\xi - \frac{e_\xi^T Q Q^T e_\xi}{\left\| e_\xi^T Q \right\|} \hat{\boldsymbol{\xi}} \boldsymbol{k}_\xi \tag{13}$$

From the above, the following equation can be obtained

$$\begin{aligned} \dot{e}_v &= \boldsymbol{A}e_v + e_B\boldsymbol{\tau} + e_\xi - \boldsymbol{L}e_v \\ \dot{e}_\xi &= \dot{\hat{\xi}} - \boldsymbol{L}_\xi(\dot{e}_v - \boldsymbol{A}e_v) - \delta \end{aligned} \tag{14}$$

and

$$\dot{\hat{B}}_x = \boldsymbol{k}_B(Pe_v - Q\boldsymbol{L}_\xi e_\xi)\boldsymbol{\tau} \tag{15}$$

where $\boldsymbol{k}_\xi$ and $\boldsymbol{k}_B$ are all positive definite matrixs. At the same time, positive definite matrices P, Q, ϖ_1 and ϖ_2 satisfy the following inequalities

$$PA - PL + 2I \leq -\varpi_1 I \tag{16}$$

$$P^T P + Q^T \boldsymbol{L}_\xi^T \boldsymbol{L}^T \boldsymbol{L}\boldsymbol{L}_\xi Q - \boldsymbol{k}_\xi Q\boldsymbol{L}_\xi - Q\boldsymbol{L}_\xi \leq -\varpi_2 I \tag{17}$$

To prove the validity of the above designed observer, the Lyapunov function is designed to be

$$V_o = e_v^T P e_v + e_\xi^T Q e_\xi + \boldsymbol{k}_B^{-1} e_B^T e_B \tag{18}$$

where $e_B = \boldsymbol{B}_x - \hat{\boldsymbol{B}}_x$, α_b is positive constant. The derivative of the above equation gives

$$\begin{aligned}\dot{V}_o =& e_v^T P(\boldsymbol{A}e_v + e_B\boldsymbol{\tau} + e_\xi - \boldsymbol{L}e_v)\\ &+e_\xi^T Q(\hat{\xi} - \delta + \boldsymbol{L}_\xi \boldsymbol{A}e_v\\ &-\boldsymbol{L}_\xi(\boldsymbol{A}e_v + e_B\boldsymbol{\tau} + e_\xi - \boldsymbol{L}e_v))\\ &+\boldsymbol{k}_B^{-1}e_B^T(-\boldsymbol{k}_B(Pe_v - Q\boldsymbol{L}_\xi e_\xi)\boldsymbol{\tau})\end{aligned} \tag{19}$$

According to Young's inequality there is the following inequality,

$$\begin{aligned}e_v^T Pe_\xi + e_\xi^T Q\boldsymbol{L}_\xi \boldsymbol{L}e_v \leq& 2e_v^T e_v + e_\xi^T P^T Pe_\xi\\ &+e_\xi^T Q\boldsymbol{L}_\xi \boldsymbol{L}\boldsymbol{L}_\xi^T \boldsymbol{L}^T Q^T e_\xi\end{aligned} \tag{20}$$

Substituting the equations (13) and (15-16) into (19) can be collated to give

$$\begin{aligned}\dot{V}_o \leq& e_v^T(PA - PL + 2I)e_v\\ &+e_\xi^T(P^T P - \boldsymbol{k}_\xi Q\boldsymbol{L}_\xi - Q\boldsymbol{L}_\xi)e_\xi\\ &+e_\xi^T(Q^T \boldsymbol{L}_\xi^T \boldsymbol{L}^T \boldsymbol{L}\boldsymbol{L}_\xi Q)e_\xi\end{aligned} \tag{21}$$

Finally, according to (16-17) have

$$\dot{V}_o \leq -\varpi_1 e_v^T e_v - \varpi_2 e_\xi^T e_\xi \tag{22}$$

The above equation shows that the observer is designed so that the estimation error for the uncertain part of the whole system can converge asymptotically.

B. DESIGN AND ANALYSIS OF AN ADAPTIVE SLIDING-MODE FAULT-TOLERANT CONTROLLER

This section proposes a fault-tolerant controller that guarantees the tracking task with prescribed transient and steady-state performance even in the event of an actuator failure for the parametric-strict-feedback non-linear system. This prescribed performance function ensures that any initial value error converges in a fixed amount of time and the detection function detects the occurrence of a fault while pre-relaxing the error bound range.

The performance function with fixed-time convergence properties is chosen as [21]

$$p(t) = \begin{cases}(p_0 - p_\infty)(\frac{T_p - t}{T_p})^{n+2} + p_\infty, & 0 \leq t < T_p\\ p_\infty, & t > T_p\end{cases} \tag{23}$$

where p_0 and p_∞ are positive constants, which are the initial and minimum values of the performance function respectively.

Remark 5: According to [14], a detection function μ can be obtained. In order to be able to limit the tracking error to a prescribed range even after a failure, we define $p_\infty = k_p\mu$ and k_p is a positive constant.

Based on the condition (4) for the above prescribed performance function, a time-varying boundary function with the following prescribed performance is designed, as described below

$$\dot{\bar{\delta}}(t) = -\bar{\lambda}_a \bar{\delta}^{\iota_a}(t) - \bar{\lambda}_b \bar{\delta}^{\iota_b}(t) \tag{24}$$

$$\dot{\underline{\delta}}(t) = -\underline{\lambda}_a \underline{\delta}^{\iota_a}(t) - \underline{\lambda}_b \underline{\delta}^{\iota_b}(t) \tag{25}$$

where $0 < \iota_b < 1$ and $\iota_a > 1$, $\bar{\lambda}_{a,b}$ and $\underline{\lambda}_{a,b}$ are the rate of change of the boundary function and is a positive constant. According to Lemma 1 and (8), we define $T_2 = max\{\frac{1}{\underline{\lambda}_a(1-\iota_a)} + \frac{1}{\underline{\lambda}_b(1-\iota_b)}, \frac{1}{\bar{\lambda}_a(1-\iota_a)} + \frac{1}{\bar{\lambda}_b(1-\iota_b)}\}$.

Remark 6: Where T_2 is the time for the target error with any initial value to arrive within the range of the performance function. Before T_2, we can not guarantee that the error is within the prescribed performance function range, which is the advantage of this method, but also the disadvantage. However, we use the advantage of fixed time convergence to compensate for this deficiency. After T_2, the proof of the PPC method we designed is basically the same as the proof of the existing works [4], [5], [6], [7], [8].

Then, define x_{1d} is the desired trajectory of the tracking and the tracking error as

$$\begin{aligned}e_{x1} &= x_1 - x_{1d}\\ \dot{e}_{x1} &= \frac{x_e\dot{x}_e + y_e\dot{y}_e}{e_{x1}}\end{aligned} \tag{26}$$

where $e_{x1} = \sqrt{x_e^2 + y_e^2}$, $x_e = x - x_d$, $y_e = y - y_d$, $e_\psi = \psi - \psi_d$, $x_e = e_{x1}cos(\psi_d)$, $y_e = e_{x1}sin(\psi_d)$.

$$\psi_d = \begin{cases}\frac{\pi}{2}[1 - sgn\,(x_e)]sgn\,(y_e) + \arctan\left(\frac{y_e}{x_e}\right), & e_{x1} \neq 0\\ \psi_d e_{x1} = 0\end{cases} \tag{27}$$

According to (9) the derivative of the error transformation function $T(e_{x1}^*)$ as follows,

$$\dot{T}(e_{x1}^*) = \begin{cases}\frac{\dot{e}_{x1}^*(\bar{\delta}(t)^2 + (e_{x1}^*)^2) - 2e_{x1}^*\bar{\delta}(t)\dot{\bar{\delta}}(t)}{(\bar{\delta}(t)^2 - (e_{x1}^*)^2)^2}, & e_{x1}^*(0) > 0\\ \frac{2e_{x1}^*\underline{\delta}(t)\dot{\underline{\delta}}(t) - \dot{e}_{x1}^*((e_{x1}^*)^2 + \underline{\delta}(t)^2)}{((e_{x1}^*)^2 - \underline{\delta}(t)^2)^2}, & e_{x1}^*(0) \leq 0\end{cases} \tag{28}$$

where z_1 is the conversion error and $\dot{e}_{x1}^* = \frac{\dot{e}_{x1}\rho(t) - e_{x1}\dot{\rho}(t)}{\rho^2(t)}$, $\dot{z}_1 = \dot{T}(e_{x1}^*)$.

The sliding surface for adaptive fault-tolerant control based on Lemma 2 can be designed as

$$S_z = z_1 - F(z_1) \tag{29}$$

The derivative of the sliding surface when $e_{x1}^* > 0$ is

$$\begin{aligned}\dot{S}_z =& -\frac{(\bar{\delta}(t)^2 + e_{x1}^{*2})\dot{\rho}(t)}{(\bar{\delta}(t)^2 - (e_{x1}^*)^2)\rho(t)^2}e_{x1}\\ &-\frac{2e_{x1}^*\bar{\delta}(t)\dot{\bar{\delta}}(t)}{(\bar{\delta}(t)^2 - (e_{x1}^*)^2)^2} - \dot{F}(z_1)\\ &+\frac{\bar{\delta}(t)^2 + e_{x1}^{*2}}{(\bar{\delta}(t)^2 - (e_{x1}^*)^2\rho(t)}(cos(\psi_d)\dot{x}_e + sin(\psi_d)\dot{y}_e)\end{aligned} \tag{30}$$

where the forcing function $F(z_1) = \eta(1 - tanh(t))$; $tanh(t) = (e^t - e^{-t})/(e^t + e^{-t})$ and $\eta = z_1(0)$. According to system (1), we have $x_e = ucos(\psi) - vsin(\psi)cos(\phi) - \dot{x}_d$ and

$y_e = usin(\psi) + vcos(\psi)cos(\phi) - \dot{y}_d$. Rectifying (30) gives

$$\begin{aligned}\dot{S}_z=&\frac{(\bar{\delta}(t)^2+e_{x1}^{*2})}{((e_{x1}^*)^2-\bar{\delta}(t)^2)\rho(t)}(\frac{e_{x1}\dot{\rho}(t)}{\rho(t)}+\dot{x}_d cos(\psi_d)+\dot{y}_d sin(\psi_d))\\&+\frac{\bar{\delta}(t)^2+e_{x1}^{*2}}{(\bar{\delta}(t)^2-(e_{x1}^*)^2\rho(t)}(ucos(e_\psi)+vsin(e_\psi)cos(\phi)\\&-\frac{2e_{x1}^*\bar{\delta}(t)\dot{\bar{\delta}}(t)}{(\bar{\delta}(t)^2-(e_{x1}^*)^2)^2}-\dot{F}(z_1)\end{aligned}\tag{31}$$

where $u = e_u + u_d$, e_u is the surge velocity error, u_d is the virtual control value for velocity is designed as follows

$$\begin{aligned}u_d=&[\dot{x}_d cos(\psi_d)+\dot{y}_d sin(\psi_d)+\frac{(\bar{\delta}(t)^2-(e_{x1}^*)^2)\rho(t)}{\bar{\delta}(t)^2+e_{x1}^{*2}}\\&(\frac{(\bar{\delta}(t)^2+e_{x1}^{*2})\dot{\rho}(t)}{((\bar{\delta}(t)^2-(e_{x1}^*)^2)\rho(t))^2}e_{x1}-\frac{2e_{x1}^*\bar{\delta}(t)\dot{\bar{\delta}}(t)}{(\bar{\delta}(t)^2-(e_{x1}^*)^2)^2}\\&-a_z S_z^{1+k_s}-b_z S_z^{1-k_s}-\dot{F}(z_1))]cos^{-1}(e_\psi)\\&-vsin(e_\psi)cos(\phi)cos^{-1}(e_\psi)\end{aligned}\tag{32}$$

The Lyapunov function is designed as

$$V_s=\frac{1}{2}S_z^2\tag{33}$$

bringing the designed virtual control value (32) into (31), while simplifying the derivative of (33), have,

$$\begin{aligned}\dot{V}_s&=S_z(\frac{\bar{\delta}(t)^2+e_{x1}^{*2}}{(\bar{\delta}(t)^2-(e_{x1}^*)^2)\rho(t)}e_2-a_z S_z^{1+k_s}-b_z S_z^{1-k_s})\\&\le -a_z S_z^{2+k_s}-b_z S_z^{2-k_s}+\frac{\bar{\delta}(t)^2+e_{x1}^{*2}}{(\bar{\delta}(t)^2-(e_{x1}^*)^2)\rho(t)}e_u\|S_z\|\\&=-a_z V_s^{1+k_s/2}-b_z V_s^{1-k_s/2}+\frac{\bar{\delta}(t)^2+e_{x1}^{*2}}{\bar{\delta}(t)^2-(e_{x1}^*)^2}\frac{e_u}{\rho(t)}V_s^{1/2}\\&=\vartheta_z e_u-a_z V_s^{1+k_s/2}-b_z V_s^{1-k_s/2}\end{aligned}\tag{34}$$

where $\vartheta_z(z_1,\bar{\delta}(t))=\frac{\bar{\delta}(t)^2+e_{x1}^{*2}}{\rho(t)(\bar{\delta}(t)^2-(e_{x1}^*)^2)^2}V_s^{1/2}$ and $\vartheta > 0$.

Similarly design and analyse the controller for yew angle,

$$\begin{aligned}r_d=&\dot{\psi}_d+\frac{(\bar{\delta}_\psi^2-(e_\psi^*)^2)\rho_\psi}{\bar{\delta}_\psi^2+e_\psi^{*2}}(\frac{(\bar{\delta}_\psi^2+e_\psi^{*2})\dot{\rho}_\psi}{((\bar{\delta}_\psi^2-(e_\psi^*)^2)\rho_\psi)^2}e_\psi\\&-\frac{2e_\psi^*\bar{\delta}_\psi\dot{\bar{\delta}}_\psi}{(\bar{\delta}_\psi^2-(e_\psi^*)^2)^2}-\dot{F}_\psi-a_\psi S_\psi^{1+k_\psi}-b_\psi S_\psi^{1-k_\psi})\end{aligned}\tag{35}$$

where $r_d = r - r_e$ is the virtual control value of yew velocity and r_e is the error.

The derivative of Lyapunov function for the sliding of yew angle as

$$\dot{V}_\psi \le \vartheta_\psi r_e - a_\psi V_\psi^{1+k_\psi/2}-b_\psi V_\psi^{1-k_\psi/2}\tag{36}$$

where $\vartheta_\psi(e_\psi,\bar{\delta}_\psi)=\frac{\bar{\delta}_\psi^2+e_\psi^{*2}}{\rho_\psi(\bar{\delta}_\psi^2-(e_\psi^*)^2)^2}V_\psi^{1/2}$. $0 < k_\psi < 1$, $a_\psi > 0$, $b_\psi > 0$, $\bar{\delta}_\psi$ is the boundary function of e_ψ^*, e_ψ^* is the conversion error of e_ψ for yew angle.

According to Lemma 1, (34) and (36), it is clearly known that it is only after the velocity error is converged to near the origin that the Trajectory tracking error converges to near the origin in a fixed time $t_s = 2(a_z + b_z)/k_s a_z b_z$, $t_\psi = 2(a_\psi + b_\psi)/k_\psi a_\psi b_\psi$.

The next step is to design an adaptive sliding mode fault-tolerant controller according to (1) to ensure that the position and velocity states of the whole closed-loop system tracking the desired objectives.

$$\begin{aligned}\dot{\boldsymbol{e}}_2&=\boldsymbol{A}\boldsymbol{v}+f(\boldsymbol{\eta},\boldsymbol{v})+\boldsymbol{B}_x\boldsymbol{\tau}+\boldsymbol{\xi}-\dot{\boldsymbol{x}}_{2d}\\&=\dot{\hat{\boldsymbol{v}}}+e_v-\dot{\boldsymbol{x}}_{2d}\end{aligned}\tag{37}$$

where the $\boldsymbol{e}_2 = [u_e, v_e, r_e]^T$ is the errors of the surge, sway, roll and yaw velocity, $\boldsymbol{B}_x = [b_u, b_v, b_r]^T$ is the health estimate value of actuators as time-varying parameters. Similarly, the estimate of the overall uncertainty component of the system is $\boldsymbol{\xi} = [\xi_u, \xi_v, \xi_r]^T$. According to (21), e_v is eventually converging to near the origin. The above equation is described as follows

$$\begin{aligned}\dot{u}_e&=\hat{b}_u\tau_u+f_u+\hat{\xi}_u-\dot{u}_d\\\dot{r}_e&=\hat{b}_r\tau_r+f_r+\hat{\xi}_r-\dot{r}_d\end{aligned}\tag{38}$$

The barrier Lyapunov function that guarantees that the surge speed error is within δ_u is as follows

$$\begin{aligned}V_{bu}&=(\delta_u^2-e_u^2)^{-\frac{1}{2}}\\V_{br}&=(\delta_r^2-e_r^2)^{-\frac{1}{2}}\end{aligned}\tag{39}$$

Remark 7: An integral form of the barrier Lyapunov function is used in [22] and [16], while a logarithmic form is used in [14]. These functions are too cumbersome in their derivation, and a novel (with a simple structure and effective) barrier Lyapunov function is chosen in this paper to limit the state errors. Also, this form allows a smaller range of limits to be found based on the detection function in [14], making the bound design more reasonable.

The derivative of the (39) is

$$\begin{aligned}\dot{V}_{bu}&=(\delta_u^2-e_u^2)^{-\frac{3}{2}}e_u(\hat{b}_u\tau_u+f_u+\hat{\xi}_u-\dot{u}_d)\\\dot{V}_{br}&=(\delta_r^2-e_r^2)^{-\frac{3}{2}}e_r(\hat{b}_r\tau_r+f_r+\hat{\xi}_r-\dot{r}_d)\end{aligned}\tag{40}$$

the controller designed in this paper is as follows:

$$\begin{aligned}\tau_u=&\hat{b}_u^{-1}(-f_u+\dot{u}_d-\hat{\xi}_u+(\delta_u^2-e_u^2)^{\frac{3}{2}}\\&(\vartheta_z-a_u V_{bu}^{1+k_u}/e_u-b_u V_{bu}^{1-k_u}/e_u))\\\tau_r=&\hat{b}_r^{-1}(-f_r+\dot{r}_d-\hat{\xi}_r+(\delta_r^2-e_r^2)^{\frac{3}{2}}\\&(\vartheta_\psi-a_r V_{br}^{1+k_r}/e_r-b_r V_{br}^{1-k_r}/e_r))\end{aligned}\tag{41}$$

where δ_u, δ_r, a_u, a_r, b_u, b_r, k_u, k_r are all positive constants.

Bringing controllers (41) into (40) has

$$\begin{aligned}\dot{V}_{bu}&\le -a_u V_{bu}^{1+k_u/2}-b_u V_{bu}^{1-k_u/2}\\\dot{V}_{br}&\le -a_r V_{br}^{1+k_r/2}-b_r V_{br}^{1-k_r/2}\end{aligned}\tag{42}$$

According to Lemma 1 and (35), it is clearly known that the velocity errors are converged to near the origin in a fixed time $t_u = 2(a_u + b_u)/k_u a_u b_u$, $t_r = 2(a_r + b_r)/k_r a_r b_r$.

TABLE 1. Main parameters for tracking of the ACV.

Variable	Value	Units
m	40000	kg
I_z	$1.8 * 10^6$	kgm^2
I_x	$2.5 * 10^5$	kgm^2
k_d	$diag\{3.1, 1.16, 0, 0.12\}$	null
k_ξ	$diag\{0.55, 0.51, 0, 0.02\}$	null
k_B	$diag\{0.2, 0, 0, 0.28\}$	null
p_0, p_∞, T_p	$diag\{300, 50, 200\}$	null
$\{\bar{\lambda}_a, \bar{\lambda}_b, \iota_a\}$	$diag\{2.1, 1.5, 2.5\}$	null
$\{\underline{\lambda}_a, \underline{\lambda}_b, \iota_b\}$	$diag\{3, 3.5, 0.2\}$	null
$\{a_z, b_z, k_s\}$	$diag\{0.09, 0.03, 0.2\}$	null
$\{a_\psi, b_\psi, k_\psi\}$	$diag\{0.03, 0.03, 0.2\}$	null

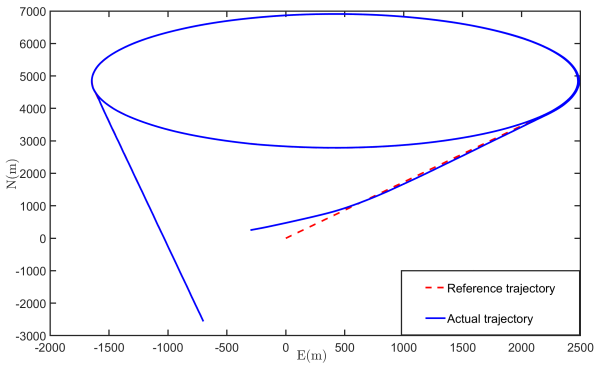

FIGURE 3. Trajectory tracking curve of the ACV in NEE coordinates.

IV. SIMULATION RESULTS

The simulation data in this paper consists of two parts. The first part verifies whether the adaptive fault-tolerant controller with PPF designed in this paper can still converge in fixed-time when the initial value of the tracking error is larger than the initial value of the performance function. At the same time verifies whether the system state error can still be limited to the designed range after a fault occurs.

The detailed modeling of the ACV is detailed in [22]. The total time for simulation is 1800s. The reference signal r_d is designed in this paper as

$$r_d = \begin{cases} 0 & t \le 240, t > 1400 \\ 0.01/57.3(t-240) rad/s & 240 < t \le 1400 \end{cases} \tag{43}$$

The reference signal of the surge velocity is $u_d = 35 knots$, the reference values for the other states are obtained from the following equation

$$\begin{aligned} \dot{x}_d &= u_d cos\psi_d \\ \dot{y}_d &= u_d sin\psi_d \\ \dot{\psi}_d &= r_d \end{aligned} \tag{44}$$

where the initial value of the reference state designed from the mentioned above first order differential equation is $x_d(0) = 0m$, $y_d(0) = 0m$, $\phi_d(0) = 0rad$, $\psi_d(0) = 50/57.3rad$, $u_d(0) = 0knots$, $v_d(0) = 0knots$, $p_d(0) = 0rad$. The initial values of the state of the ACV's kinematic model in this part are chosen as $x(0) = -300m$, $y(0) = 250m$, $\phi(0) = 0$, $\psi = 35°$, $u(0) = 35knots$, $v(0) = 0knots$, $p(0) = 0°$, $r(0) = 0°/s$,$\bar{\delta}(0) = 1.30$, $\underline{\delta}_u(0) = 1.20$, $\bar{\delta}_u = 35.02$, $\underline{\delta}_u = 5.83$, $\bar{\delta}_v = 5.83$, $\underline{\delta}_v = 5.83$. $\bar{\delta}_r = 5.83$, $\underline{\delta}_r = 5.83$.

Environmental disturbances and fault messages are separately designed as $\boldsymbol{\xi} = \{10sin(5t) + 0.2sin(0.05t), 5cos(3t), 3cos(2t)\}$, $B_x = \begin{cases} diag\{1, 0, 0, 1\}, & t \le 800s \\ diag\{0.6 + 0.01sin(2t), & \\ 0, 0, 0.8 + 0.01sin(3t)\}, & t > 800s \end{cases}$.

The main parameters of the system and detailed parameters of the controller in this section for tracking of the ACV are given as shown in Table 1.

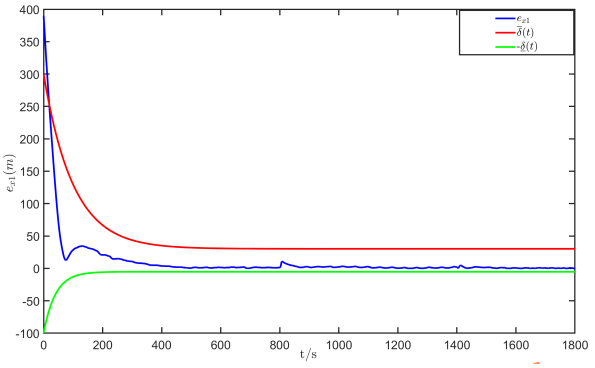

FIGURE 4. The position tracking error curve with the controller designed in this paper.

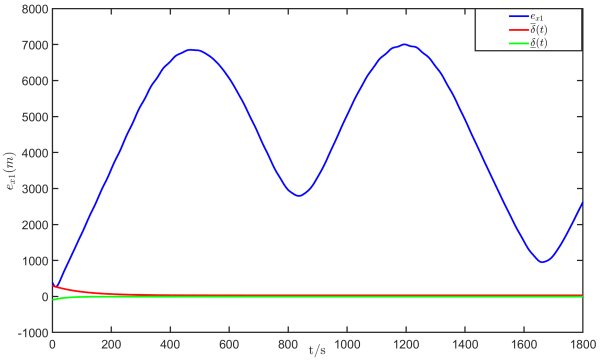

FIGURE 5. The position tracking error curve with the controller designed in [12].

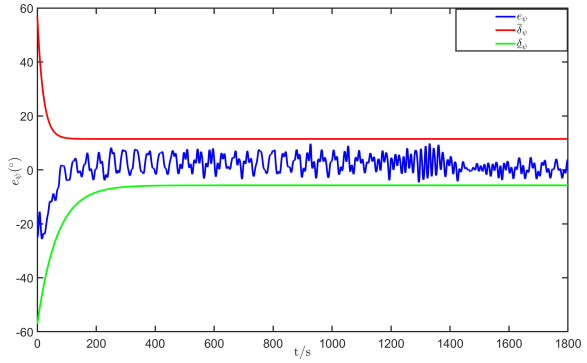

FIGURE 6. The yew angle error curve with the controller designed in this paper.

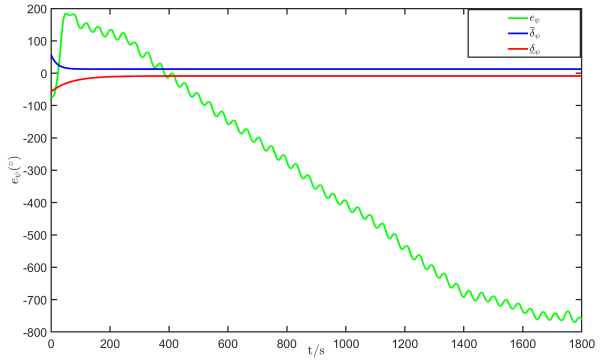

FIGURE 7. The yew angle error curve with the controller designed in [12].

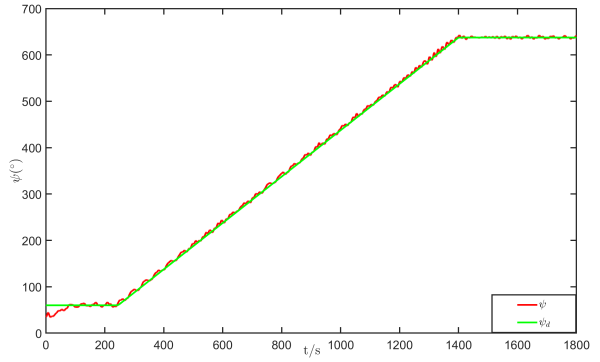

FIGURE 8. Time response curve for yaw angle of the ACV.

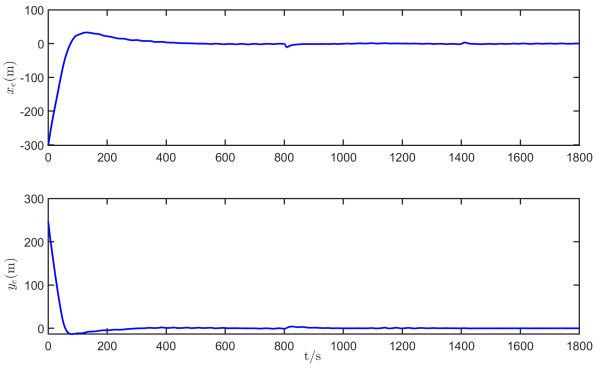

FIGURE 9. Time response curves for tracking errors of surge and sway position of the ACV.

It can be obtained from the results in Fig.2, Figs.7-8 that the control system proposed in this paper accomplishes the task of tracking the trajectory and heading angle of the hovercraft relatively well. At the same time, it has good robustness after a fault occurs. Fig.3, Fig.5 and Fig.9 mainly depict whether the tracking error of the system state is limited to a predetermined range. From the results, it can be seen that the system status error are well limited to the pre-set range even when the initial value is larger than the boundary. The simulation results in Fig.4 and Fig.6 mainly use the control system proposed in [12]. The PPF designed in this controller

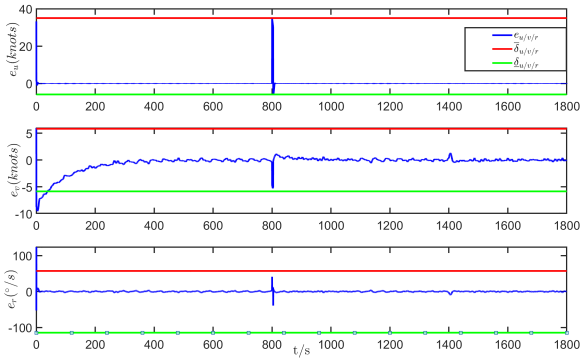

FIGURE 10. The tracking error curve for the surge, sway and yaw velocity of the ACV.

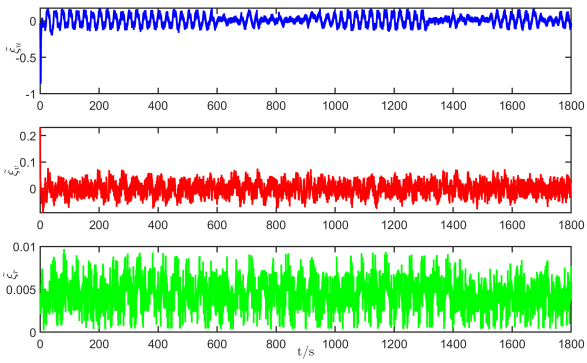

FIGURE 11. Time response curves for estimation errors of ξ.

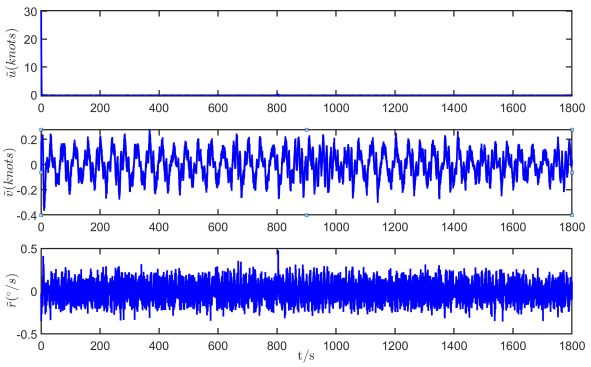

FIGURE 12. Time response curves of the system state estimation error for the integrated observer.

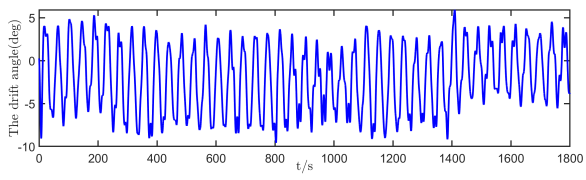

FIGURE 13. Time response curves of the drift angle.

is of a general form with initial value constraints, so the controller is unstable when the initial value of the state error

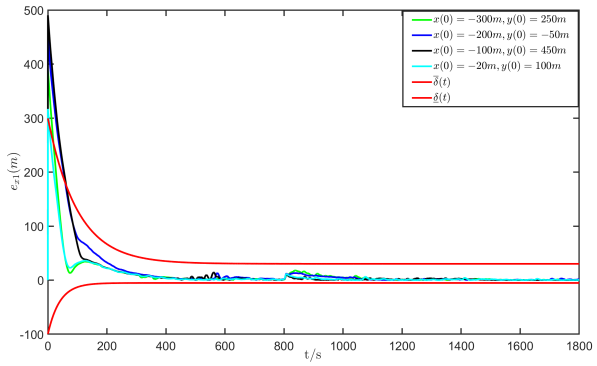

FIGURE 14. Time response curves for position tracking errors with different initial values.

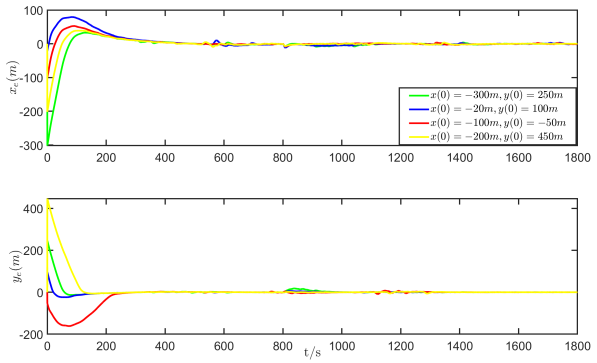

FIGURE 15. Time response curves for surge and sway position errors with different initial values.

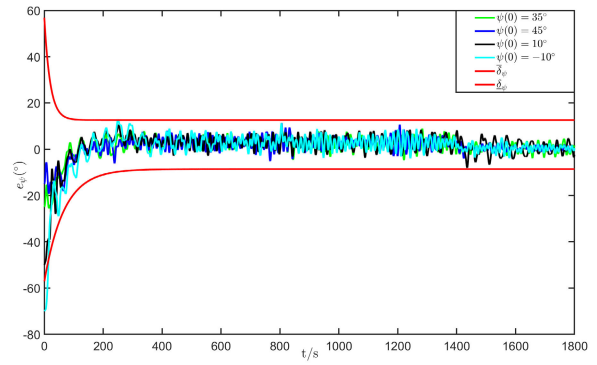

FIGURE 16. Time response curves for yaw angle error with different initial values.

is out of bounds. The comparison results from Figs.3-6 verify the advantages of the fault-tolerant controller with the new PPF designed in this paper. Fig.10 and Fig.11 show mainly the time profiles of the estimation errors of the state and intermediate variables of the integrated observer. The results verify the validity of the observer. Fig.12 is the time response curve for the drift angle, which is within the safe range allowed for the high speed of the ACV.

Then the simulation results in Figs.13-15 demonstrate that the controller designed in this paper can guarantee that the tracking error can converge in a fixed time for different initial values. The initial values of the state of the ACV's kinematic model are chosen as $x(0) = -300m$, $y(0) = 250m$, $\psi(0) = 35°$, $x(0) = -20m$, $y(0) = 100m$, $\psi(0) = 45°$,$x(0) = -100m$, $y(0) = -50m$, $\psi(0) = 10°$,$x(0) = -200m$, $y(0) = 450m$, $\psi(0) = -10°$.

V. CONCLUSION

This paper proposes an adaptive fault-tolerant controller based on a new prescribed performance function. The main focus is to improve the transient performance of the Trajectory tracking control of ACV, provided that system stability in the presence of actuator faults and environmental disturbances is also ensured. The proposed new prescribed performance function is no longer limited by the initial value and is more suitable for applications in hovercraft tracking control with particular operating environments. The method incorporates an observer that does not require perturbation upper bound information, improving the overall system robustness and reducing the stress on the controller. The performance function used has the advantage of fixed-time convergence, further ensuring the transient performance of the ACV's tracking control. Transient performance is critical to the safety of ACV that often travel at high speeds in complex environments. Due to the large mass and high speed of ACV, failures such as stalling and actuator saturation occur frequently. Further improvements to the fragility performance of the PPC method after failure saturation of the ACV will therefore be considered in future work inspired by [7] and [8].

APPENDIX A
CREDIT AUTHORSHIP CONTRIBUTION STATEMENT

Fu Mingyu: Software, Resource. Bai Dan: Conceptualization, Methodology,Writing-original draft. Deng Hanbo:Writing-review.

REFERENCES

[1] W. Xie, D. Cabecinhas, R. Cunha, and C. Silvestre, "Robust motion control of an underactuated hovercraft," *IEEE Trans. Control Syst. Technol.*, vol. 27, no. 5, pp. 2195–2208, Sep. 2019.

[2] M. Fu, D. Bai, H. Deng, and L. Dong, "A novel GSMC-based ACV trajectory tracking under unknown disturbance upper bound and time-varying model coefficients," *Int. J. Control, Autom. Syst.*, vol. 21, no. 8, pp. 1115–1123, Mar. 2023.

[3] K. Zhao, Y. Song, C. L. P. Chen, and L. Chen, "Adaptive asymptotic tracking with global performance for nonlinear systems with unknown control directions," *IEEE Trans. Autom. Control*, vol. 67, no. 3, pp. 1566–1573, Mar. 2022.

[4] X. Bu and B. Jiang, "Fragility-free prescribed performance control without approximation applied to waverider aerocraft," *IEEE J. Miniaturization Air Space Syst.*, early access, Feb. 6, 2023, doi: 10.1109/jmass.2023.3242304.

[5] X. Bu, B. Jiang, and H. Lei, "Low-complexity fuzzy neural control of constrained waverider vehicles via fragility-free prescribed performance approach," *IEEE Trans. Fuzzy Syst.*, early access, Oct. 26, 2022, doi: 10.1109/tfuzz.2022.3217378.

[6] Z. Ren and T. Xia, "Fixed-time output feedback distributed cooperative event-triggered control for multiple surface vessels with prescribed performance constraints," *IEEE Access*, vol. 11, pp. 15198–15210, 2023.

[7] X. Bu, B. Jiang, and H. Lei, "Performance guaranteed finite-time non-affine control of waverider vehicles without function-approximation," *IEEE Trans. Intell. Transp. Syst.*, vol. 24, no. 3, pp. 3252–3262, Mar. 2023, doi: 10.1109/TITS.2022.3224424.

[8] X. Bu, B. Jiang, and H. Lei, "Nonfragile quantitative prescribed performance control of waverider vehicles with actuator saturation," *IEEE Trans. Aerosp. Electron. Syst.*, vol. 58, no. 4, pp. 3538–3548, Aug. 2022.
[9] J.-X. Zhang, Q.-G. Wang, and W. Ding, "Global output-feedback prescribed performance control of nonlinear systems with unknown virtual control coefficients," *IEEE Trans. Autom. Control*, vol. 67, no. 12, pp. 6904–6911, Dec. 2022.
[10] J.-X. Zhang and G.-H. Yang, "Prescribed performance fault-tolerant control of uncertain nonlinear systems with unknown control directions," *IEEE Trans. Autom. Control*, vol. 62, no. 12, pp. 6529–6535, Dec. 2017.
[11] C. P. Bechlioulis and G. A. Rovithakis, "Robust adaptive control of feedback linearizable MIMO nonlinear systems with prescribed performance," *IEEE Trans. Autom. Control*, vol. 53, no. 9, pp. 2090–2099, Oct. 2008.
[12] Y. Wang, H. Wang, and M. Fu, "Prescribed performance trajectory tracking control of dynamic positioning ship under input saturation," *Trans. Inst. Meas. Control*, vol. 44, no. 1, pp. 30–39, Jan. 2022.
[13] M. Fu, T. Zhang, F. Ding, and D. Wang, "Adaptive fixed-time trajectory tracking control for underactuated hovercraft with prescribed performance in the presence of model uncertainties," *Complexity*, vol. 2021, pp. 1–18, Apr. 2021, doi: 10.1155/2021/6677445.
[14] H. Ouyang and Y. Lin, "Adaptive fault-tolerant control for actuator failures: A switching strategy," *Automatica*, vol. 81, no. 18, pp. 87–95, Jul. 2017.
[15] H.-B. Sun, G.-D. Zong, J.-W. Cui, and K.-B. Shi, "Fixed-time sliding mode output feedback tracking control for autonomous underwater vehicle with prescribed performance constraint," *Ocean Eng.*, vol. 247, no. 18, pp. 673–689, 2022.
[16] H. Liu, B. Meng, and X. Tian, "Finite-time prescribed performance trajectory tracking control for underactuated autonomous underwater vehicles based on a tan-type barrier Lyapunov function," *IEEE Access*, vol. 10, pp. 53664–53675, 2022, doi: 10.1109/ACCESS.2022.3175854.
[17] X. Gao, J.-X. Zhang, and L. Hao, "Fault-tolerant control of pneumatic continuum manipulators under actuator faults," *IEEE Trans. Ind. Informat.*, vol. 17, no. 12, pp. 8299–8307, Dec. 2021.
[18] T. N. Truong, A. T. Vo, and H.-J. Kang, "A backstepping global fast terminal sliding mode control for trajectory tracking control of industrial robotic manipulators," *IEEE Access*, vol. 9, pp. 31921–31931, 2021.
[19] Z. Lin, H. D. Wang, M. Karkoub, U. H. Shah, and M. Li, "Prescribed performance based sliding mode path-following control of UVMS with flexible joints using extended state observer based sliding mode disturbance observer," *Ocean Eng.*, vol. 240, Nov. 2021, Art. no. 109915, doi: 10.1016/j.oceaneng.2021.109915.
[20] H. Liang, Y. Fu, J. Gao, and H. Cao, "Finite-time velocity-observed based adaptive output-feedback trajectory tracking formation control for underactuated unmanned underwater vehicles with prescribed transient performance," *Ocean Eng.*, vol. 233, Aug. 2021, Art. no. 109071, doi: 10.1016/j.oceaneng.2021.109071.
[21] K. Zhao, Y. Song, T. Ma, and L. He, "Prescribed performance control of uncertain Euler–Lagrange systems subject to full-state constraints," *IEEE Trans. Neural Netw. Learn. Syst.*, vol. 29, no. 8, pp. 3478–3489, Aug. 2018.
[22] M.-Y. Fu, L.-J. Dong, Y.-J. Xu, and D. Bai, "A novel asymmetrical integral barrier Lyapunov function-based trajectory tracking control for hovercraft with multiple constraints," *Ocean Eng.*, vol. 263, no. 29, pp. 112–132, Aug. 2022.
[23] K. Zhang, B. Jiang, X. Yan, Z. Mao, and M. M. Polycarpou, "Fault-tolerant control for systems with unmatched actuator faults and disturbances," *IEEE Trans. Autom. Control*, vol. 66, no. 4, pp. 1725–1732, Apr. 2021, doi: 10.1109/TAC.2020.2997347.
[24] L. Zhang, H. Liu, D. Tang, Y. Hou, and Y. Wang, "Adaptive fixed-time fault-tolerant tracking control and its application for robot manipulators," *IEEE Trans. Ind. Electron.*, vol. 69, no. 3, pp. 2956–2966, Mar. 2022.
[25] H. Wang, S. Wu, and Q. Wang, "Global sliding mode control for nonlinear vehicle antilock braking system," *IEEE Access*, vol. 9, pp. 40349–40359, 2021.
[26] I. S. Dimanidis, C. P. Bechlioulis, and G. A. Rovithakis, "Output feedback approximation-free prescribed performance tracking control for uncertain MIMO nonlinear systems," *IEEE Trans. Autom. Control*, vol. 65, no. 12, pp. 5058–5069, Dec. 2020.
[27] A. Polyakov, "Nonlinear feedback design for fixed-time stabilization of linear control systems," *IEEE Trans. Autom. Control*, vol. 57, no. 8, pp. 2106–2110, Aug. 2012.
[28] Y.-S. Lu and J.-S. Chen, "Design of a global sliding-mode controller for a motor drive with bounded control," *Int. J. Control*, vol. 62, no. 5, pp. 1001–1019, Feb. 2007.

MINGYU FU was born in 1964. She received the M.S. and Ph.D. degrees from the College of Automation, Harbin Engineering University, Harbin, China, in 1988 and 2005, respectively. She is currently a Professor and a Ph.D. Supervisor with Harbin Engineering University. Her current research interests include hovercraft motion control, the automatic control of the unmanned surface vehicle, and vessel dynamic positioning control.

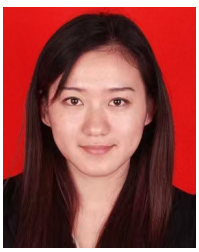

DAN BAI was born in 1990. She is currently pursuing the Ph.D. degree in control science and engineering with Harbin Engineering University, Harbin, China. Her current research interests include hovercraft motion control, vessel autonomous driving systems, and underactuated ship motion control.

HANBO DENG was born in Harbin, China, in 1988. He is currently pursuing the Ph.D. degree in control science and engineering with Harbin Engineering University, Harbin.